Meat Science 199 (2023) 109126

Contents lists available at ScienceDirect

Meat Science

journal homepage: www.elsevier.com/locate/meatsci

Integrating identification and targeted proteomics to discover the potential indicators of postmortem lamb meat quality

Caiyan Huang [a,b], Christophe Blecker [b], Li Chen [a], Can Xiang [a], Xiaochun Zheng [a], Zhenyu Wang [a,*], Dequan Zhang [a,*]

[a] Institute of Food Science and Technology, Chinese Academy of Agriculture Sciences, Key Laboratory of Agro-Products Quality & Safety Harvest, Storage, Transportation, Management and Control, Ministry of Agriculture and Rural Affairs, Beijing 100193, China
[b] University of Liège, Gembloux Agro-Bio Tech, Unit of Food Science and Formulation, Avenue de la Faculté d'Agronomie 2, Gembloux B-5030, Belgium

ARTICLE INFO

Keywords:
Meat quality
Proteomics
Protein indicators
Glycolysis
Oxidative phosphorylation
Muscle contraction

ABSTRACT

The aim of this study was to identify the potential indicators of lamb meat quality by TMT and PRM-based proteomics combined with bioinformatic analysis. Lamb muscles were divided into three different meat quality groups (high, middle and low) according to tenderness (shear force, MFI value), colour (a^* value, R630/580), and water-holding capacity (cooking loss, drip loss) at 24 h postmortem. The results showed that the abundance of phosphoglycerate kinase 1 (PGK1), β-enolase (ENO3), myosin-binding protein C (MYBPC1) and myosin regulatory light chain 2 (MYLPF) was significantly different in the three groups and could be used as potential indicators to characterize meat quality. Moreover, the postmortem processes of glycolysis, oxidative phosphorylation, and muscle contraction remarkably changed in different groups, and were the key biological pathways influencing meat quality. Overall, this study depicted the proteomic landscape of meat that furthers our understanding of the molecular mechanism of meat quality and provides a reference for developing non-destructive detection technology for meat quality.

1. Introduction

Lamb meat is an important source of animal products for human nutrition. It provides a good source of high-quality protein, essential amino acids, omega-3 fatty acids, vitamins (vitamin B6, B12) and minerals (phosphorus, iron, and zinc, etc.) (Willimas, 2007). According to Food and Agriculture Organization (FAO) figures, the global production of lamb meat was approximately 336.64 million tons in 2019 (http://www.fao.org/faostat/zh/#data/QCL). Meat quality is an essential prerequisite for consumer acceptability and industrial profitability, which includes meat tenderness, colour, water holding capacity (WHC) and flavour (Huang et al., 2020). Currently, high-quality meat demands have been increasing with higher living standards and increasing incomes, which has become a hot issue of global concern in the field of meat science. Meat quality deterioration mainly consists of discolouration, high drip loss and texture deterioration of meat in postmortem or retail displays. However, the loss or waste of meat caused by the deterioration of meat quality traits accounts for approximately 20% per year, according to FAO's report (http://www.fao.org/3/i4807e/i4807e.pdf), which leads to a huge waste for meat resources, environmental pollution, and economic loss. Biomarkers or indicators are molecular compositions of biological processes that reveal the differential expression associated with the phenotype of a specific trait (Huang et al., 2020; Wu, Fu, Therkildsen, Li, & Dai, 2015). Thus, confirmation of indicators related to meat quality is the material basis for identifying and regulating postmortem meat quality, which is also the key link to study meat quality change and to provide control technologies. Therefore, it is necessary to confirm the key meat quality indicators that could characterize and affect lamb meat quality in postmortem, and develop the accurate regulation and control technologies to evaluate and improve meat quality.

Postmortem aging of muscle is an intricate biological process that involves physical and biochemical changes at the cellular level. For almost twenty years, several studies have reported the possible biological pathways that can affect meat quality attributes during the conversion of muscle to meat postmortem. For example, glycolysis

* Corresponding authors at: Institute of Food Science and Technology, Chinese Academy of Agricultural Sciences, No.2 Yuanmingyuan West Road, Haidian District, Beijing 100193, PR China.
E-mail addresses: food2006wzy@163.com (Z. Wang), dequan_zhang0118@126.com (D. Zhang).

https://doi.org/10.1016/j.meatsci.2023.109126
Received 16 August 2022; Received in revised form 14 December 2022; Accepted 19 January 2023
Available online 23 January 2023

(Chauhan & England, 2018), calpain system (Koohmaraie & Geesink, 2006), heat shock proteins (Ma & Kim, 2020), apoptosis (Zhang et al., 2013) and post-translational protein modification (Li et al., 2021) were investigated. Despite this research progress, the key substances characterizing meat quality traits are still unknown and it remains a large percentage of low-quality meat production without available targeted control. Furthermore, the application of proteomics to discover potential biological markers related to meat quality attributes has become a possible approach to solve this problem in the field of meat science (Huang et al., 2020; Wu et al., 2015; Wu, Fu, et al., 2015). Proteins can be considered the building blocks and functional executors of the cell and tissue. Therefore, in-depth research of the proteome of lamb meat will lay a foundation for comprehensively understanding the molecular mechanisms during muscle to meat conversion, and better guide treatment to reduce the production of inferior meat in the industry.

The objective of this study was to identify the differentially abundant proteins related to lamb meat quality in three different lamb meat quality traits (DLMQTs) groups by the tandem mass tag (TMT)-10plex labelling-based proteomics. Then, for the subsequent validation phase, parallel reaction monitoring (PRM) targeted proteomics and western blotting approaches were used to further confirm the key potential protein indicators of postmortem lamb meat quality. These data resources will reveal a map of molecular changes related to lamb quality, to better understand the molecular mechanism of meat quality degradation and provide a reference for regulating and controlling postmortem lamb meat quality.

2. Materials and methods

2.1. Sample collection

One hundred 6 to 8 month-old Tan sheep (male) from ten batches were supplied by Ningxia Yanchi Tan Sheep Industry Development Group Co., Ltd., China (with the same feeding patterns). All sheep were slaughtered according to the cutting technical specification of mutton (NY/T 1564–2007, the ministry of agriculture of the People's Republic of China, 2007). Ten sheep were slaughtered per day for ten consecutive days. A total of 100 left *Longissimus thoracis* (LT) lamb muscles (hot carcass weight: 20.09 ± 1.69 kg) were collected within 45 min after bleeding. The samples were displayed in the air and wrapped with oxygen-permeable polyethylene (PE)-film with an oxygen transmission rate of 10,600 cm^3/ (m^2·24 h·atm) and moisture transmission amount of 68.5 g/ (m^2·24 h), and stored at a chilling room (2 ± 2 °C) in the slaughterhouse. After 24 h, the pH, shear force, meat colour (a* and R630/580), cooking loss and drip loss of the fresh LT muscle samples were measured immediately. Meanwhile, about 200 g samples were retrieved at 24 h postmortem and immediately preserved in liquid nitrogen, and then stored at −80 °C until processing.

One hundred muscle samples were clustered into 3 different meat quality groups (Group1, Group2 and Group3, n = 3 x 6 = 18 samples) according to the tenderness (shear force and MFI), colour (a^* value and R630/580) and WHC (cooking loss and drip loss) of lamb meat at 24 h postmortem. Group 1 with the higher a* value, R630/580, MFI, and the lower shear force, drip loss and cooking loss; Group 2 with the middle a* value, R630/580, MFI, shear force, drip loss and cooking loss; and Group 3 with the lower a* value, R630/580, MFI, and the higher shear force, drip loss and cooking loss. The procedure was considered as a full-randomized block design with slaughter day as a blocking factor. The experimental unit (LT muscle) was considered as a plot and hot carcass weight was distorting variation sources controlled by the experimental design in order to minimize the residual variation.

2.2. Meat quality traits analysis

2.2.1. pH value

A portable pH meter (Testo 205 pH meter, Lenzkirch, Germany) was used for the detection of pH value. The probe was inserted 2 cm into the meat, and each sample with the three technical replicates. Before each set of recordings, the pH meter was calibrated at the chilling room (average temperature above 2 °C) using pH 4.0 and pH 7.0 buffers.

2.2.2. Shear force and cooking loss

We utilized the method from the previous literature (Hopkins, Toohey, Warner, Kerr, & van de Ven, 2010), with little modification. The samples were weighed (about 65 g), and cooked for 35 min at 71 °C in the waterbath with a thermoregulator and a 1500 W heating element (HH-4, Weipinyiqi, Shenzheng, China) and then blotted dry with filter paper and reweighed. One hundred muscle samples were cooked in ten cooking batches, and 10 muscle samples were allocated to each batch. When the samples cooled at 4 °C for one night and determined the shear force using a tenderometer (C-LM4, Northeast Agricultural University, Harbin, China), muscle samples were cut with 1 cm × 1 cm × 1.5 cm cube, and each sample with the ten technical replicates. The cooking loss percentage was calculated using the following formula:

$$Cooking\ loss\% = \frac{Raw\ weight - Cooking\ weight}{Raw\ weight} \times 100\%$$

2.2.3. Myofibrillar fragmentation index (MFI)

The MFI was conducted as previously described (Rajagopal & Oommen, 2015). 1 g sample was homogenized for 30 s using Ultra TurraxT10 (IKA Labortechnik, Staufen, Germany) in the 10-fold volume of ice-cold extraction buffer (100 mmol/L KCl, 20 mmol/L K_2HPO_4, 1 mmol/L EDTA, 1 mmol/L $MgCl_2$, 1 mmol/L NaN_3), and repeated three times with an interval of 60 s on the ice. And then, the tissue homogenate was centrifugated (Neofuge 15R, Heal Force, Shanghai, China) at 3000 g for 15 min at 4 °C. The precipitate was suspended in a 2.5-fold volume of ice-cold extraction buffer for 15 s, and the myofibril suspension was thinned with the extraction buffer to adjust the protein concentration of 0.5 mg/mL. The diluted samples were added into 96-well seahorse plates (Corning®, No.3599, New York, USA) and detected their absorbance at 540 nm using the microplate reader (Multimode Microplate Reader, Spark®, Tecan, Switzerland). MFI value was obtained by multiplying the absorbance value at 540 nm with 200.

2.3. a* value and R630/580

Meat colour measurements were performed on fresh samples at 24 h postmortem of storage at 4 °C. Meat colour value was evaluated after 45 min of blooming at 4 °C by Minolta CM-600D spectrophotometer (Konica Minolta Sensing Inc., Osaka, Japan). An aperture size of 8 mm with a D65 illuminant and a 10° standard observer were used throughout the experiment. The a^* value reading from the average of four sites randomly selected on the surface of each fresh cut sample, visible fat and connective tissue were avoided. The CIE L^*, a^* and b^* readings and reflectance values from 360 nm to 740 nm at 10 nm intervals were used to characterize the surface colour. The ratio of reflectance at 630 to 580 nm (R630/580) was computed as a measurement of the surface meat colour stability.

2.3.1. Drip loss

The measurement of drip loss was performed according to previous literature (Jin et al., 2021). About 10 g sample of meat (0.5 cm × 5 cm × 10 cm) was collected with the direction of muscle fibers and weighed, which was suspended in a polythene bag at 4 °C chilling room. After 24 h, the sample was soaked up by filter paper and reweighed. The drip loss percentage was calculated below:

$$Loss\ drip(\%) = \frac{W1 - W2}{W1} \times 100\%$$

Where W1 represents the initial weight (g) of muscle sample, W2 represents the sample end weight after the loss of natural dripping water

at 4 °C for 24 h.

2.4. Proteomics data acquisition

2.4.1. Protein extraction and tryptic digestion

The muscle samples were lysed in SDT buffer (100 mM Tris-HCl, 4% SDS, 1 mM DTT, pH 7.6) with protease inhibitor cocktail (R0278, Sigma, USA), and homogenized twice for 60 s (FastPrep-24, MP Biomedicals, USA) with arenaceous quartz and ceramic sphere. Subsequently, samples for ten times ultrasonic wave extraction, 10 s one time with a recess of 15 s, which were heated in a boiling water bath for 15 min and centrifugated at 14,000 g for 40 min to take away the tissue residue. The supernatants were filtered by 0.22 μm membrane and collected filtrate, and then the concentration of protein was detected by the BCA Protein Assay Kit (Thermo Fisher Scientific Inc. Waltham, MA). Dithiothreitol (DTT) was added into the extracted protein with a final concentration of 100 mM and heated in a boiling water bath for 5 min. After cooling down to room temperature, UA buffer (150 mM Tris-HCl, 8 M Urea, pH 8.0) was added to the protein solutions and centrifugated at 14,000 g for 15 min to remove the detergent, DTT and other low molecular weight components by repeated ultrafiltration (Microcon units, 10 kD). And then, iodoacetamide (IAA) (100 mM IAA in UA buffer) was added to block reduced cysteine residues and the samples were incubated for 30 min in darkness at room temperature, and centrifugated at 14,000 g for 15 min. The filters were rinsed with UA buffer three times and then 100 mM triethylammonium bicarbonate (TEAB) buffer twice by centrifugation (14,000 *g*, 15 min). Finally, the suspensions of protein were digested with trypsin (Promega) in a proportion of 1:50 at 37 °C for 16 h, and then desalted by Sep-Pak C18 cartridges (Empore™ SPE, Sigma, USA) as well as vacuum-dried using Speed Vac.

2.4.2. TMT labelling

After C18 washing, 100 μg of peptides from each of the 18 muscle samples were taken for the following TMT-10plex labelling-based proteomics analysis. Two samples were mixed with an equal number of peptides from the same groups. And then using TMT-10plex label reagents to label the nine peptide samples according to the manufacturer's specifications (Thermo Fisher Scientific, San Jose, USA).

2.4.3. Peptide pre-fractionation by high-pH HPLC

Labelled peptide samples fractionated using High pH Reversed-Phase Peptide Fractionation Kit (Thermo Fisher Scientific Inc. Waltham, MA). The differentially-labelled peptides were equally mixed and redissolved in 0.1% trifluoroacetic acid solution and loaded into the equilibrated. Subsequently, under the condition of the aqueous phase, the peptides were combined with the hydrophobic resin and desalted by washing the column with water using low speed centrifugation. Finally, a step gradient of increasing acetonitrile concentrations in a high pH elution buffer was then loaded to the columns to elute binding peptide samples in 10 different fractions gathered by centrifugation. The collected fractions were desalted by C18 cartridges (Empore™ SPE, Sigma, USA), and were vacuum centrifuged to dryness and reconstituted in 12 μL Milli-Q water with 0.1% formic acid (FA).

2.4.4. LC-MS/MS

The labelled peptides were analyzed by LC-MS/MS system with a Q Exactive mass spectrometer (Thermo Scientific) that was combined with EASY-nLC (Thermo Scientific) for 60 min. Redissolved peptide samples were loaded into a reverse-phase trap column (Thermo Scientific Acclaim PepMap100 nano-Viper C18, 100 μm × 2 cm,), and linked with the C18 reversed phase analytical column (Thermo Scientific Easy Column, 75 μm × 10 cm) in 0.1% FA solution and isolated by a linear gradient of solution (84% acetonitrile and 0.1% FA) with the flow rate of 300 nL/min gathered using IntelliFlow approach. MS worked at a positive-ion-mode. The MS data were obtained with a data-dependent mode selecting dynamically the precursor ions from the survey scan (300–1800 m/z) for the higher energy collisional dissociation (HCD) fragmentation. The resolution of MS1 was set to 70,000 (200 m/z). the automatic gain control (AGC) target was set to 3e6, the maximum injects time to 50 ms, and the dynamic exclusion duration was 40 s. MS2 resolution for HCD spectra was set to 17,500 (200 m/z), and isolation width was 2 m/z, normalized collision energy was 30 eV and the underfill ratio was 0.1%.

2.5. PRM analysis

According to the data analysis results for TMT labelling-based proteomics, 18 targets proteins of interest (ENO1, ENO3, PKM, PGM1, NDUFB9, NDUFA4, UQCRH, UQCRQ, CYC1, NDUFA2, NDUFB7, MYLK2, LOC101113001, TPM2, TTN, TNNI1, TNNC1, MYL1) were verified by PRM targeted proteomics. The experiment's strategy was the same as the TMT labelling-based proteomics. Adding the independent retention time peptides into the samples. 200 μg proteins from each of the 18 tissue samples were prepared for the following PRM targeted proteomics detection. Subsequently, the nine samples were digested as described above, and the solvent of the peptides was 0.1% FA in water. We took the same number of peptides from each sample and mixed the suitable dosage of stable isotope internal standard peptide. 1 μg peptide was taken from each sample and mixed with 20 fmol standard peptides (Pierce™ Peptide Retention Time Calibration Mixture, NO. 88320, Thermo Scientific) for detection by high performance liquid chromatography (HPLC) system (Thermo Scientific). Buffer A was 0.1 FA in water and buffer B was 0.1% FA with 84% acetonitrile in water. Samples were separated at 300 nL/min across a linear gradient ranging from 5% - 10% buffer B in 2 min, and then from 10% to 30% buffer B in 43 min followed by a sharp increase to 100% buffer B in 5 min, and then maintained for 10 min. The separated samples were analyzed by Q-Exactive HF (Thermo Scientific) for 60 min in the positive ion detection mode. MS1 scanning range and resolution were set to 300–1800 m/z and 60,000 (200 m/z), respectively. MS2 resolution was set to 30,000 (200 m/z) and the normalized collision energy (NCE) setting as 27. The raw data of PRM were analyzed by skyline software (version 3.5.0).

2.6. Western blotting analysis

To extract the proteins from the lamb muscles, 18 LT muscle samples were minced and lysed on ice by RIPA lysis buffer (Sigma, USA) added to protease inhibitor cocktail (Sigma, USA), and then the protein concentration was determined by the BCA Protein Assay Kit (Thermo Fisher Scientific Inc. Waltham, MA). Equal amounts of the protein lysates were separated by 10% of separating gel and 4% of stacking gel of SDS-PAGE and transferred to the PVDF blotting membrane (Millipore, Darmstadt, Germany). PVDF membranes were blocked with 5% nonfat dry milk in TBST solution (137 mM NaCl, 20 mM Tris, 0.1% Tween-20), PVDF membranes were incubated and put up 4 °C for the night overnight with the following first antibodies: PGK1 (AV48140, 1:1000, Sigma-Aldrich, St. Louis, MO), ENO2 (A12341, 1:1000, ABclonal, Wuhan, China), MYLPF (ab79935, 1:1000, Abcam Inc., Cambridge, MA), MYBPC1 (ab124196, 1:1000, Abcam Inc., Cambridge, MA), ACTB (SAB2100037, 1:1000, Sigma-Aldrich, St. Louis, MO), TNNI2 (A7937, 1:1000, ABclonal, Wuhan, China), CAPZB (SAB2500193, 1:1000, Sigma-Aldrich, St. Louis, MO), NDUFV3 (ab272584, 1:1000, Abcam Inc., Cambridge, MA), COX6A2 (ab110264, 1:1000, Abcam Inc., Cambridge, MA), LOC101114379 (A3976, 1:1000, ABclonal, Wuhan, China), GAPDH (AB-M-M001, 1:500, Goodhere Bio, Hangzhou, China), β-Tubulin (abs137976, 1:5000, Abcam Inc., Cambridge, MA), And then the PVDF membranes were incubated with the appropriate secondary antibody (goat anti-mouse IgG H&L (HRP), ab6789, 1:2000, Abcam Inc., Cambridge, MA or goat anti-rabbit IgG H&L (HRP), AS014, 1:1000, ABclonal, Wuhan, China) for 80 min at room temperature. Finally, the bands were tested by an ECL detection kit (Bio-Rad, Hercules, USA) and captured on a ChemiDocTMMP imaging system (UVP, Upland, CA,

USA). The relative abundance of each band was calculated by normalizing with GAPDH/β-Tubulin using the Quantity One software (version 4.62, Bio-Rad).

2.7. Bioinformatics analysis

Log_2(fold change) was performed by the mean of proteins abundance ratio in LT lamb muscle among three DLMQTs groups (Group 1/Group 2, Group 1/Group 3, and Group 2/Group 3). *t*-test was analyzed for each couple of groups to be compared ($P < 0.05$). The criteria for significantly differential abundance proteins choice were that the *P* value should be <0.05 and |Log_2(fold change) | (Log_2(FC)) should be more than log_2(1.2). Protein data were processed and analyzed with the freely available MaxQuant search engine and searched in the Uniprot database of Ovis_aries_63813_20201207.fasta (https://www.uniprot.org/uniprot). InterProScan software version 5.36–75 was performed to find the protein domain signatures. Blast2 GO software was used to analyze GO enrichment analysis. KGEE pathway analysis of differential abundance proteins were performed using the online Kyoto Encyclopedia of Genes and Genomes (KEGG) database (http://geneontology.org/). Fisher' exact test was applied to find the enrichment analysis, and only functional categories and pathways with *P* values <0.05 were considered as significant. The protein-protein interaction (PPI) information of 54 differential abundance proteins was performed to find their gene symbols by STRING software version 11.5 (http://string-db.org/). The results were downloaded in the XGMML format and imported into Cytoscape software version 3.8.2 (http://www.cytoscape.org/).

2.8. Statistical analysis

Statistical analysis was carried out by IBM-SPSS Statistics Software (version 26.0, IBM, Armonk, NY, USA). The linear mixed model (LMM) was considered to determine significant differences with DLMQTs groups as the fixed effect and random effects for slaughter day, and hot carcass weight as covariate. All lamb meat quality traits (pH, MFI, a^* value, R630/580, cooking loss and drip loss) and the relative abundance of differential proteins was modelled in similar fashion. For shear force and cooking loss, models included fixed effect for DLMQTs groups and random effects for slaughter day, shear force test date and cooking batches, and hot carcass weight as covariate. The predicted means were compared using a least significance differences (LSD) level of 5%. The GraphPad Prism (version 9), Origin (version 2021b) and R (version 4.1.2) were used to draw graphics. The results were expressed as mean ± standard error.

Refer to the predecessors' analysis methods (Starkey, Geesink, Collins, Hutton Oddy, & Hopkins, 2016; Starkey, Geesink, van de Ven, & Hopkins, 2017), the mixed models were performed using ASReml-R (Butler, 2009) within the R software environment (R Core Team, 2014) to make the prediction models for meat quality traits. There were six different models used for identifying the relationships with each model containing the covariates of PGK1, PGM1, ENO3, PKM, NDUFA2, NDUFB7, TPM2, TTN, TNNI1, TNNC1, MYL1, MYBPC1 and MYLPF. Slaughter day and hot carcass weight as the random terms were included in all models. Moreover, shear force test date and cooking batches are also the random terms for Model 1 and Model 5. The models are as follows:

Model 1: Shear force = PGK1 + PGM1 + ENO3 + PKM + NDUFA2 + NDUFB7 + MYBPC1 + MYLPF + TPM2 + TTN + TNNI1 + TNNC1 + MYL1 + slaughter day + hot carcass weight + cooking batches + shear force test date.

Model 2: MFI = PGK1 + PGM1 + ENO3 + PKM + NDUFA2 + NDUFB7 + MYBPC1 + MYLPF + TPM2 + TTN + TNNI1 + TNNC1 + MYL1 + slaughter day + hot carcass weight.

Model 3: a^* = PGK1 + PGM1 + ENO3 + PKM + NDUFA2 + NDUFB7 + MYBPC1 + MYLPF + TPM2 + TTN + TNNI1 + TNNC1 + MYL1 + slaughter day + hot carcass weight.

Model 4: R630/580 = PGK1 + PGM1 + ENO3 + PKM + NDUFA2 + NDUFB7 + MYBPC1 + MYLPF + TPM2 + TTN + TNNI1 + TNNC1 + MYL1 + slaughter day + hot carcass weight.

Model 5: Cooking loss = PGK1 + PGK1 + PGM1 + ENO3 + PKM + NDUFA2 + NDUFB7 + MYBPC1 + MYLPF + TPM2 + TTN + TNNI1 + TNNC1 + MYL1 + slaughter day + hot carcass weight + cooking batches.

Model 6: Drip loss = PGK1 + PGM1 + ENO3 + PKM + NDUFA2 + NDUFB7 + MYBPC1 + MYLPF + TPM2 + TTN + TNNI1 + TNNC1 + MYL1 + slaughter day + hot carcass weight.

Each model was simplified by using the Wald F statistic of small samples (Kenward & Roger, 1997), and the non-marginal fixed terms that were not significant at the level of 0.05 were sequentially removed (Kenward & Roger, 1997). The marginal and conditional R^2 values of six models were calculated after the non-significant items were removed (Nakagawa & Schielzeth, 2013).

3. Results

3.1. Characterization of the proteomic landscape of raw lamb meat

A total of 100 LT muscles were collected from lambs within 45 min after slaughter. The meat quality traits (pH, shear force, MFI, a^* value R630/580, drip loss and cooking loss) at 24 h postmortem were determined. Among them, three groups were selected as the different DLMQTs samples: Group 1 had a higher a^* value, R630/580, MFI, and lower shear force, drip loss and cooking loss, Group 2 had a middle a^* value, R630/580, MFI, shear force, drip loss and cooking loss, and Group 3 had a lower a^* value, R630/580, MFI, and higher shear force, drip loss and cooking loss. The differences in shear force (Fig. 1A), MFI (Fig. 1B), a^* value (Fig. 1C), R630/580 (Fig. 1D), drip loss (Fig. 1E), cooking loss (Fig. 1F) and pH value (Fig. 1G) of the three DLMQTs groups were determined at 24 h postmortem, and all meat quality indices showed a significant difference in the three DLMQTs groups ($P < 0.05$, Table S1), except for pH value ($P > 0.05$, Table S1). Hierarchical cluster analysis showed a clear stratification in the three DLMQTs groups according to the results of shear force, MFI, a^* value, R630/580, cooking loss and drip loss of lamb meat at 24 h postmortem (Fig. 1H).

Eighteen samples (Group 1, Group 2 and Group 3, $n = 6$) from the 100 LT lamb muscles were used for quantitative protein expression profiling. From these samples, 2208 proteins had a false discovery rate (FDR) <1% at the levels of peptide and protein using a TMT labelling based quantitative mass spectrum strategy. Among them, 2176 proteins were quantified in the three DLMQTs groups (Fig. 2A). For data analysis, we compared the Group 1/Group 2, Group 1/Group 3 and Group 2/Group 3 of the three DLMQTs groups, and a total of 317, 233 and 69 differentially abundant proteins (DAPs) were identified respectively, according to *t*-test adjusted ($P < 0.05$) and $|\log_2(\text{fold change})| = \log_2 FC > \log_2 1.2$ (Fig. 2B). The DAPs in Group 1/Group 2, Group 1/Group 3 and Group 2/Group 3 were analyzed using Venn diagram showed that a total of 429 proteins were discovered, of which 10 proteins were differentially expressed among the Group 1/Group 2, Group 1/Group 3 and Group 2/Group 3 (Fig. 2C). To reveal the molecular landscape and proteomics features of lamb meat, the fuzzy c-means algorithm was performed to cluster protein expression profiles in the three DLMQTs groups (Fig. 2D). Six different pattern clusters represented regulated proteins differently. Among them, cluster 2 represented that these proteins were downregulated, and cluster 5 represented that these proteins were upregulated, whereas cluster 1, cluster 3, cluster 4 and cluster 6 represented those proteins that showed a bimodal expression pattern. In addition, we performed domain, GO (Gene ontology, cellular component (CC), biological process (BP), molecular function (MF), and KEGG (Kyoto encyclopedia of genes and genomes) enrichment analyses for each cluster to reveal the molecular profile of lamb meat.

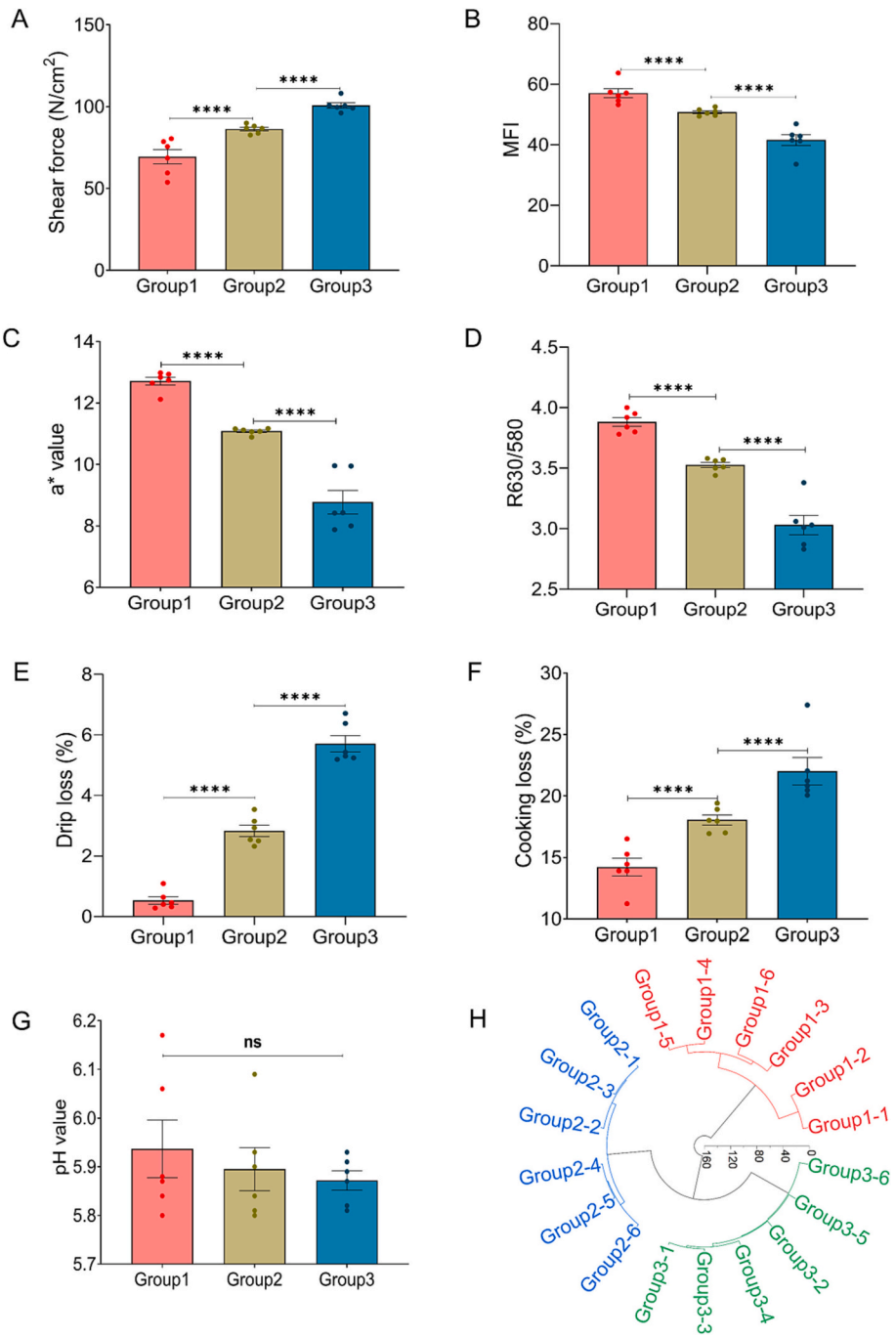

Fig. 1. Characterization of meat quality in three differential lamb meat quality traits (DLMQTs) groups at 24 h postmortem. (A) shear force, (B) MFI value, (C) a^* value, (D) R630/580, (E) drip loss, (F) cooking loss, (G) pH value, (H) Hierarchical cluster analysis for three DLMQTs groups according to shear force, MFI, a* value, R630/580, drip loss and cooking loss of lamb meat at 24 h postmortem. Predicted means and standard error bars are plotted. *P* value: * $P < 0.05$, ** $P < 0.01$, *** $P < 0.001$, **** $P < 0.0001$. Each group with 6 samples.

3.2. The key biological pathways and proteins associated with lamb meat quality

To better understand and elaborate the biological processes and the key proteins affecting the changes in lamb meat quality traits postmortem, we searched for biological pathways in the KEGG database in which the DAPs at the different levels of DLMQTs were involved. KEGG annotation indicated that the three DLMQTs groups' lamb meat proteomes were significantly enriched in regulation of actin cytoskeleton, leukocyte trans endothelial migration, thermogenesis, muscle contraction, retrograde endocannabinoid signalling, oxidative phosphorylation, diabetic cardiomyopathy, hippo signalling pathway, ribosome biogenesis in eukaryotes, glycolysis/gluconeogenesis, starch and sucrose metabolism, various types of N-glycan biosynthesis, NF-kappa B signalling pathway and cytosolic DNA-sensing pathway, NOD-like receptor signallhaveing pathway (*t*-test, *P* value <0.05) (Fig. 3A). A total of more than ten pathways were significantly changed among the Group 1/Group 2, Group 1/Group 3 and Group 2/Group 3. In particular, glycolysis, oxidative phosphorylation, and muscle contraction pathways have been reported that have a strong effect on the conversion of muscle to meat in postmortem (Hou et al., 2020; Huang et al., 2020; Yu et al., 2017; Yu et al., 2017). Therefore, we focused on the biological pathways of the differential proteins, including glycolysis, oxidative phosphorylation and muscle contraction, and 54 DAPs were involved in these pathways (Fig. 3B). To pinpoint the effects of these differential proteins on the key biological pathways and molecular functions of lamb meat and protein interactions, we performed the protein-protein interactions (PPI) and 191 interactions identified in the PPI analysis (Fig. 3C).

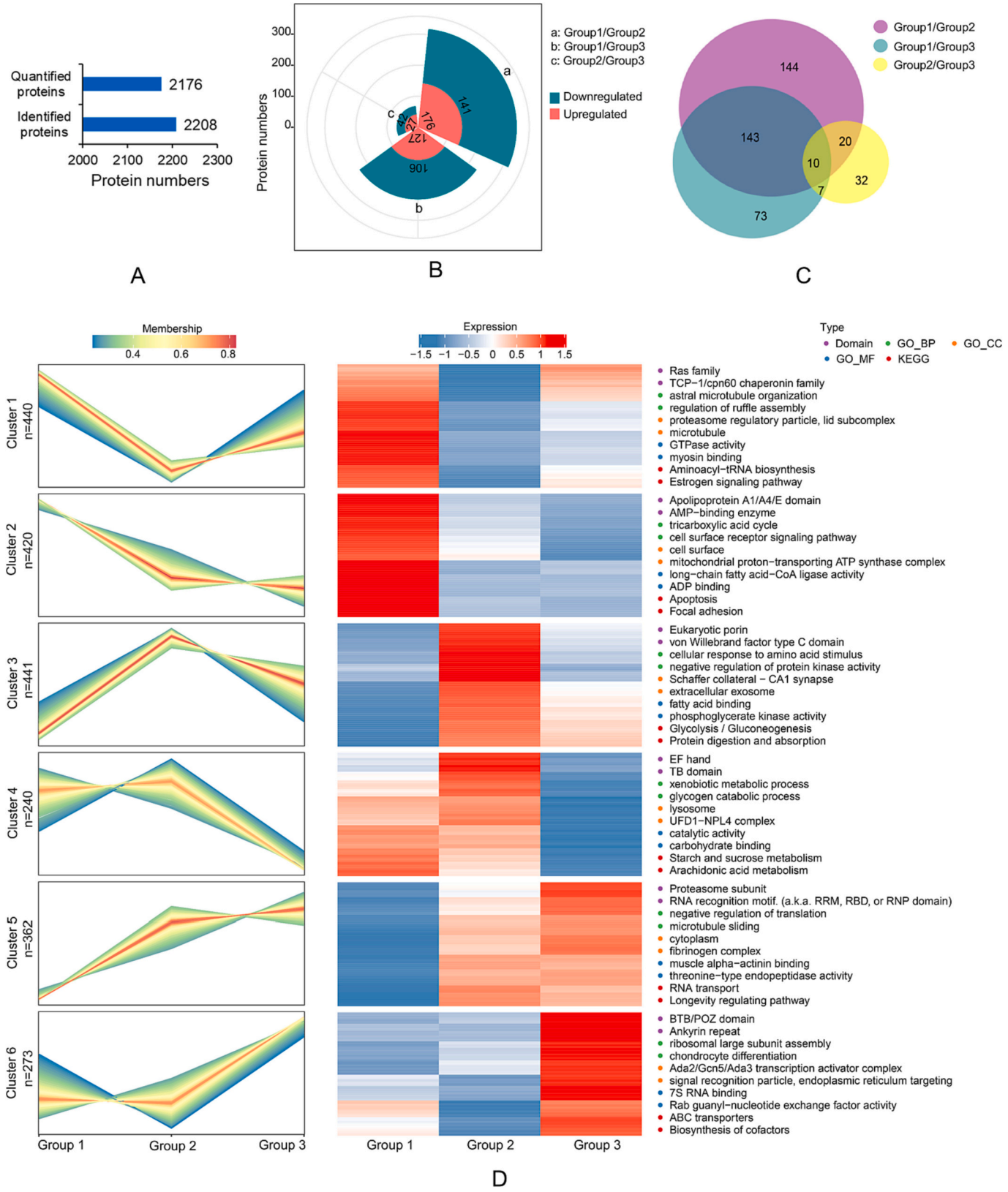

Fig. 2. The proteomic landscape of lamb meat in three DLMQTs groups. (A) The number of proteins was identified and quantified in lamb meat, respectively, (B) The significantly dysregulated proteins among the three DLMQTs groups (P value <0.05 and FC > 1.2), (C) Venn diagram of remarkably changed proteins (FC > 1.2 and $P < 0.05$) in the three DLMQTs groups, (D) 2176 quantified proteins in three DLMQTs groups were used for functional analysis by Fuzzy c-means clustering. Each group with 3 samples in Proteomics analysis (Two samples were mixed with an equal number of peptides from the same groups).

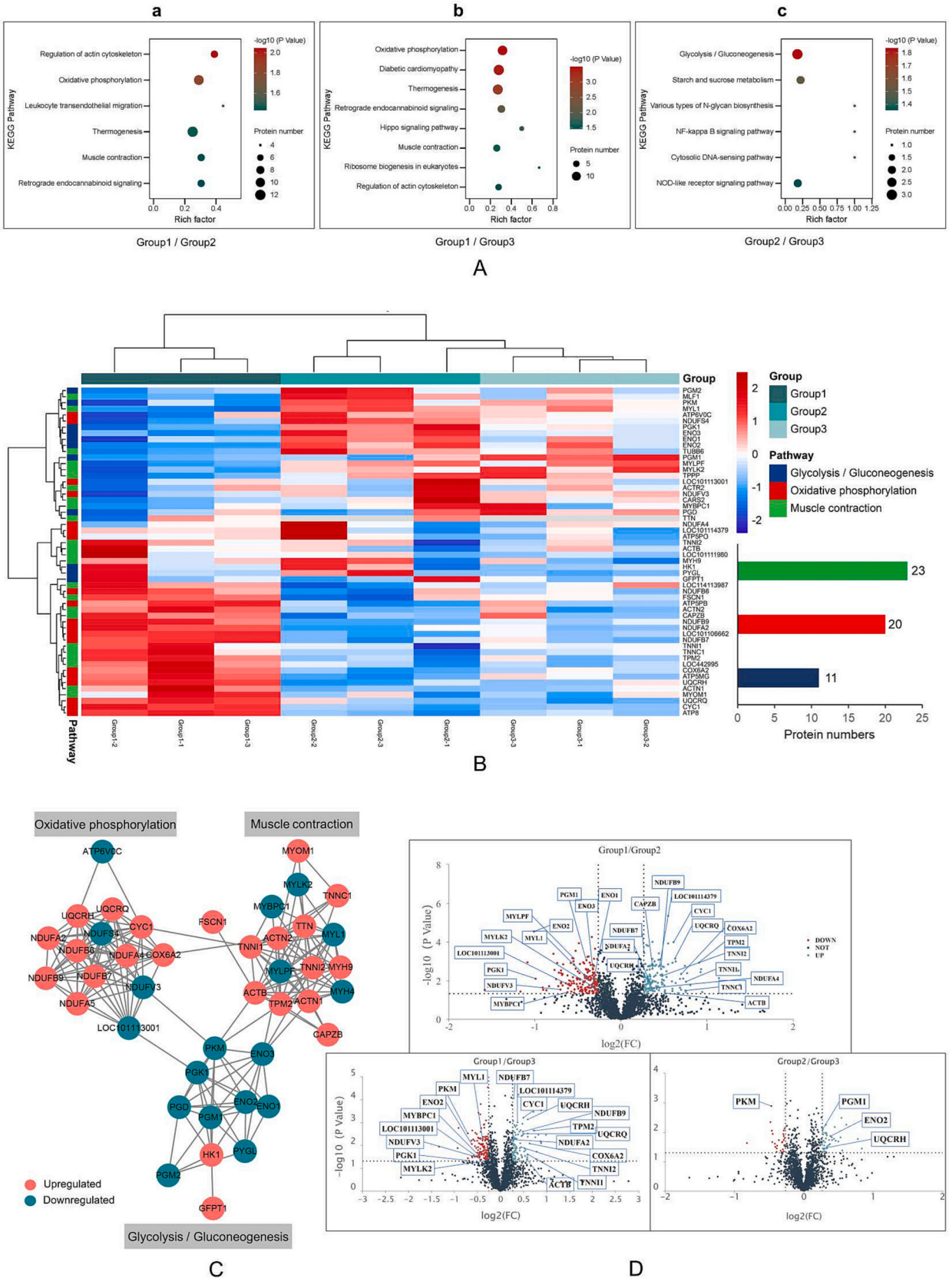

Fig. 3. KEGG pathway and protein-protein interaction analysis for the differentially abundant proteins (DAPs) related to meat quality among three DLMQTs groups. (A) A total of 429 DAPs were performed by the KEGG pathway enrichment ($P < 0.05$), (B) The heatmap of 54 key dysregulated proteins and their regulating pathways in three DLMQTs groups, (C) Protein-protein interaction analysis of the significantly dysregulated proteins taken from the STRING database were plotted as a network, only connected nodes are shown, (D) The volcano plots for mutations of the DAPs associated with meat quality. Each group with 3 samples in Proteomics analysis (Two samples were mixed with an equal number of peptides from the same groups).

Among them, a total of 11 proteins (PGK1 (phosphoglycerate kinase 1) (Silva et al., 2019), PGM1 (phosphoglucomutase 1) (Fuente-Garcia et al., 2019; Silva et al., 2019), PKM (pyruvate kinase PKM isoform X2) (Kim, Jeong, Yang, & Hur, 2019; Wu, Fu, et al., 2015; Wu, Gao, et al., 2015), ENO1 (α-enolase) (Hou et al., 2020; Huang et al., 2020), ENO3 (β- enolase) (Yu et al., 2018), MYLPF (myosin regulatory light chain 2) (Kim et al., 2019; Silva et al., 2019), MYL1 (myosin light chain 1) (Kim et al., 2019; Silva et al., 2019), TNNI2 (troponin I, fast skeletal muscle) (Kim et al., 2019; Silva et al., 2019), TNNC1 (troponin C type 1) (Beldarrain et al., 2018; Yu et al., 2018), CAPZB (F-actin-capping protein subunit beta isoform X1) (Boudon et al., 2020), TTN (titin) (Weng et al., 2021) have been reported as the differentially abundant proteins related to meat quality attributes in previous studies. In addition, 17 proteins, including ENO2 (γ-enolase), UQCRQ (complex III subunit 8), UQCRH (cytochrome *b*-c1 complex subunit 6), LOC101114379 (NADH dehydrogenase [ubiquinone] 1 alpha subcomplex subunit 5), NDUFV3 (NADH dehydrogenase [ubiquinone] flavoprotein 3, mitochondrial isoform X2), NDUFA2 (NADH dehydrogenase [ubiquinone] 1 alpha subcomplex subunit 2 isoform X1), CYC1 (cytochrome *c* domain-containing protein), NDUFB7 (complex I—B18), LOC101113001 (cytochrome *b*-c1 complex subunit), COX6A2 (cytochrome *c* oxidase subunit), NDUFA4 (NDUFA4 mitochondrial complex), NDUFB9 (NADH dehydrogenase [ubiquinone] 1 beta subcomplex subunit 9 isoform X1), TPM2 (tropomyosin beta chain isoform X1), ACTB (actin, cytoplasmic 1), MYLK2 (myosin light chain kinase 2), MYBPC1 (myosin-binding protein C) and TNNI1 (troponin I, slow skeletal muscle), showed a differential abundance among at least two DLMQTs groups ($P < 0.05$ and FC > 1.2). Therefore, these 28 DAPs may be related to lamb meat quality traits by TMT- proteomics (Fig. 3D).

3.3. Validation of potential indicators related to lamb meat quality by parallel reaction monitoring and western blotting approaches

To confirm whether 28 DAPs can be used as indicators of lamb meat quality traits, the abundance level of 18 of these 28 proteins in the three DLMQTs groups was verified using PRM targeted proteomics, while the other 10 proteins of 28 were evaluated by western blotting as the PRM was not able to identify them. First, we performed quantitative analysis of these proteins by PRM technology and the results showed the 18 proteins (ENO1, ENO3, PGM1, PKM, NDUFB9, NDUFA4, NDUFA2, NDUFB7, UQCRH, UQCRQ, CYC1, LOC101113001, TPM2, TTN, TNNI1, TNNC1, MYLK2, MYL1 in Fig. 4A. The results showed that the

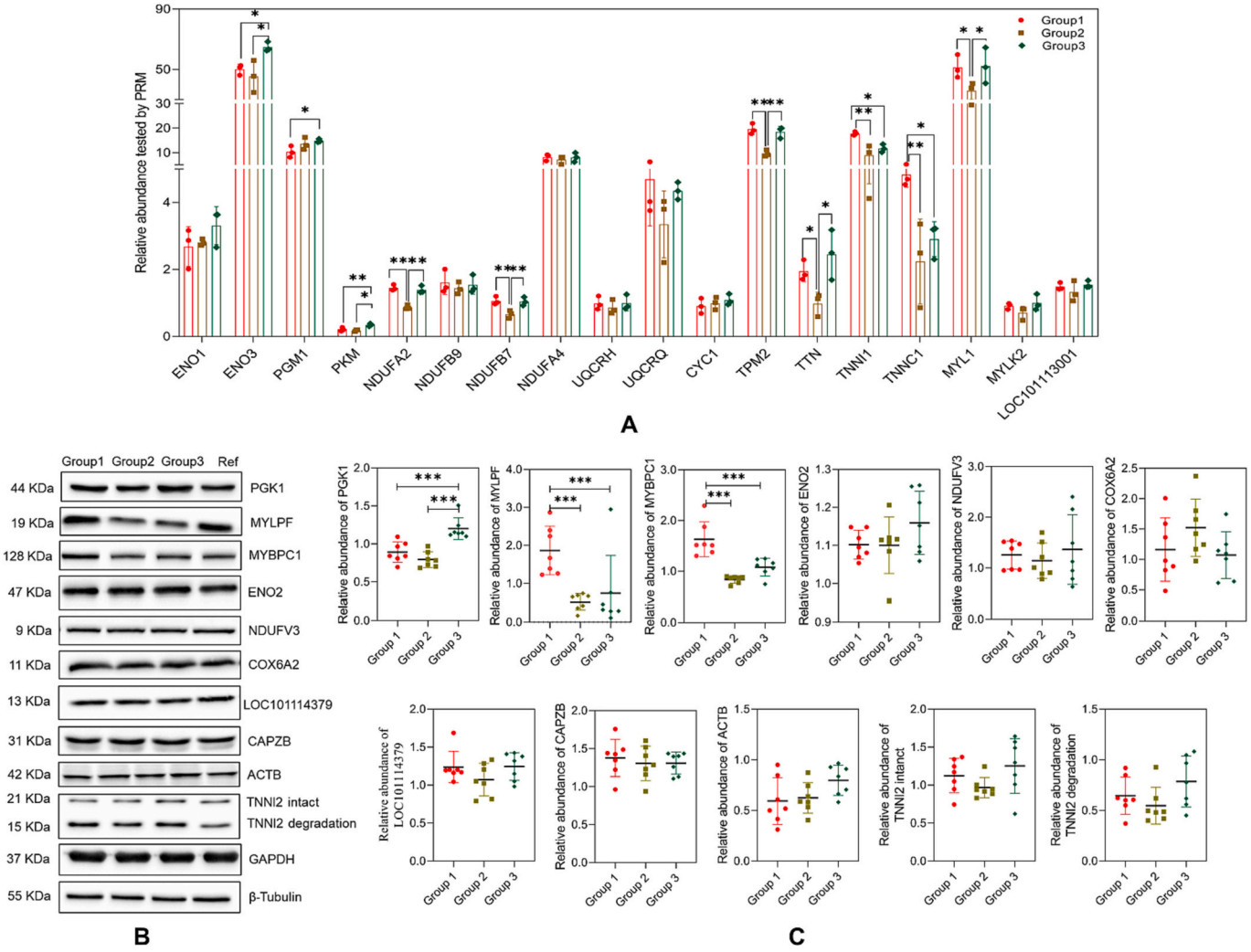

Fig. 4. Verification of the differentially abundant proteins (DAPs) by non-synthetic peptide-based parallel reaction monitoring (PRM) and western blot approaches of ten PRM-undetected proteins. (A) The abundance of 18 DAPs (ENO1, ENO3, PGM1, PKM, NDUFB9, NDUFA4, NDUFA2, NDUFB7, UQCRH, UQCRQ, CYC1, LOC101113001, TPM2, TTN, TNNI1, TNNC1, MYLK2 and MYL1) was detected by non-synthetic peptide based PRM technology, (B) Western blotting images of 10 DAPs (PGK1, ENO2, LOC101114379, NDUFV3, COX6A2, MYLPF, MYBPC1, TNNI2, CAPZB ACTB), Ref represented the standard sample (18 pooled controls for each band, (C) Abundance of 10 DAPs was performed by western blotting. Predicted means and standard error bars are plotted. *P* value: * $P < 0.05$; ** $P < 0.01$; *** $P < 0.001$. Each group with 3 samples in PRM (Two samples were mixed with an equal number of peptides from the same groups) and 6 samples in western blot analysis.

abundance level of PGM1 was strikingly different in the three DLMQTs groups ($P < 0.05$), and there was no significant difference in the other eight proteins (ENO1, NDUFB9, NDUFA4, UQCRH, UQCRQ, CYC1, MYLK2, LOC101113001) ($P > 0.05$). Moreover, the abundance of the 9 proteins (ENO3, PKM, NDUFA2, NDUFB7, TPM2, TTN, TNNI1, TNNC1, MYL1) showed a remarkable difference only between the two DLMQTs groups ($P < 0.05$). In addition, the abundance level of another 10 proteins (PGK1, ENO2, LOC101114379, NDUFV3, COX6A2, MYLPF, MYBPC1, TNNI2, CAPZB, ACTB) was detected by western blotting (Fig. 4B). The results confirmed that the abundance level of PGK1 in Group 3 was significantly higher than that in Group 1 and Group 2 ($P < 0.01$), and there was no significant difference between Group 1 and Group 2 ($P > 0.05$). The MYLPF and MYBPC1 proteins were more abundant in Group 1 than in Group 2 and Group 3 ($P < 0.01$), and there was no significant difference between Group 2 and Group 3 ($P > 0.05$, Fig. 4C). Therefore, we found that there was a significant difference in 13 dysregulated proteins (PGM1, PGK1, ENO3, PKM, NDUFA2, NDUFB7, MYBPC1, MYLPF, TPM2, TTN, TNNI1, TNNC1 and MYL1) relative abundance between the three DLMQTs groups ($P < 0.05$, Table S1). Suggesting that these 13 dysregulated proteins may related to lamb meat quality traits, which could impact lamb meat quality attributes via glycolysis, oxidative phosphorylation, and muscle contraction pathways. To define the relationship between lamb meat quality traits and 13 dysregulated proteins. Mixed models were fitted using ASReml-R within the R software environment to perform the prediction models for lamb meat quality traits (shear force and MFI, a*, R630/580, cooking loss and drip loss). As shown in Table 1, For model 1, it was found that shear force was significantly affected by PGK1, ENO3, MYBPC1, MYLPF and TPM2 ($P < 0.001$), the marginal $R^2 = 0.90$ and the conditional $R^2 = 0.92$. And the MFI value was significantly affected by PGK1, ENO3, PGM1, NDUFA2, NDUFB7, MYBPC1, MYLPF, TNNI1 and MYL1 ($P < 0.05$) in model 2, with a marginal $R^2 = 0.85$ and a conditional $R^2 = 0.87$. In addition, the PGK1, ENO3, PGM1, MYBPC1, MYLPF, TPM2, TTN, TNNI1 and TNNC1 were all significant predictors of both a^* and R630/580 in model 3 and 4 ($P < 0.001$). When individual traits were modelled (Model 5) against cooking loss, the PGK1, ENO3, PGM1, NDUFB7, MYBPC1, MYLPF, TNNI1, TNNC1 and MYL1 were significant ($P < 0.01$), the marginal $R^2 = 0.69$ and the conditional $R^2 = 0.92$. Moreover, for model 6, the results revealed that drip loss was significantly influenced by PGK1, ENO3, PGM1, NDUFA2, MYBPC1, MYLPF, TNNI1 and TNNC1 ($P < 0.001$), the marginal $R^2 = 0.87$ and the conditional $R^2 = 0.93$. Therefore, the results indicated that the postmortem lamb meat quality traits (shear force, MFI, a^* value, R630/580, cooking loss and drip loss) were significantly affected by the glycolytic enzymes (PGK1 and ENO3) and the structural proteins (MYBPC1 and MYLPF). The potential indicators were selected if they met the following criteria: (1) only proteins that have been reported can be used the potential indicators in previous studies related to meat quality traits; (2) only proteins with different abundance proteins among at least two DLMQTs groups by proteomics ($P < 0.05$); and (3) only proteins that showed a significant association with meat quality traits (general linear mixed models, $P < 0.05$). Therefore, it is suggested that PGK1, ENO3, MYBPC1 and MYLPF may be used as potential indicators affecting and determining the changes of lamb meat quality after slaughter (Fig. 5).

4. Discussion

Several studies have reported that proteomics is relevant to identify the differentially abundant proteins that genuinely reflect changes in meat quality. Moreover, proteomics can be used to understand the molecular mechanism of the conversion from muscle to meat postmortem (Huang et al., 2020; Wu, Fu, et al., 2015; Wu, Gao, et al., 2015). However, previous studies only focused on the determination of the differentially abundant proteins regarding differential meat tenderness (Beldarrain et al., 2018; Boudon et al., 2020), differential drip loss (Zhang, Wang, Xu, & Xu, 2019) or differential colour stability (Wu, Fu,

Table 1
Differentially abundant proteins which significantly affected meat quality traits (regression coefficients, standard errors and probability level).[1]

	Coefficient	Standard error	*P-value*	Marginal R^2	Conditional R^2
Model 1 – Shear force					
Intercept	92.19	7.34	***		
PGK1	−5.49	4.51	***		
ENO3	0.23	0.09	***	0.90	0.92
MYBPC1	−17.89	2.95	***		
MYLPF	−10.50	1.39	***		
TPM2	1.17	0.30	***		
Model 2 – MFI					
Intercept	58.10	6.51	***		
PGK1	−3.04	3.04	***		
ENO3	−0.10	0.07	***		
PGM1	−0.14	0.38	***		
NDUFA2	1.68	6.24	*	0.85	0.87
NDUFB7	−40.34	9.01	**		
MYBPC1	3.01	1.80	***		
MYLPF	5.83	1.11	***		
TNNI1	0.51	0.37	**		
MYL1	0.47	0.11	***		
Model 3 – a^*					
Intercept	14.60	0.99	***		
PGK1	−2.20	0.49	***		
ENO3	−0.05	0.01	***		
PGM1	0.07	0.04	***		
MYBPC1	−0.68	0.30	***	0.89	0.94
MYLPF	0.69	0.17	***		
TPM2	0.03	0.03	***		
TTN	−1.79	0.22	***		
TNNI1	−0.14	0.05	***		
TNNC1	1.64	0.24	***		
Model 4 – R630/580					
Intercept	4.33	0.20	***		
PGK1	−0.46	0.10	***		
ENO3	−0.01	0.002	***		
PGM1	0.01	0.01	***		
MYBPC1	−0.22	0.06	***	0.88	0.96
MYLPF	0.05	0.03	***		
TPM2	0.02	0.01	***		
TTN	−0.43	0.04	***		
TNNI1	−0.05	0.01	***		
TNNC1	0.46	0.05	***		
Model 5 – Cooking loss					
Intercept	27.74	3.27	***		
PGK1	−5.98	1.36	***		
ENO3	0.16	0.03	***		
PGM1	−0.11	0.18	***		
NDUFB7	17.23	3.65	***	0.69	0.92
MYBPC1	0.81	0.77	***		
MYLPF	0.78	0.53	***		
TNNI1	0.12	0.18	**		
TNNC1	−3.71	0.56	***		
MYL1	−0.36	0.05	***		
Model 6 – Drip loss					
Intercept	1.03	1.01	***		
PGK1	−0.24	0.51	***		
ENO3	0.10	0.01	***		
PGM1	0.04	0.05	***		
NDUFA2	−3.31	0.67	***	0.87	0.96
MYBPC1	−0.01	0.27	***		
MYLPF	−0.11	0.19	***		
TTN	2.08	0.26	***		
TNNI1	0.09	0.07	***		
TNNC1	−1.19	0.24	***		

[1] *P* value: * $P < 0.05$, ** $P < 0.01$, *** $P < 0.001$.

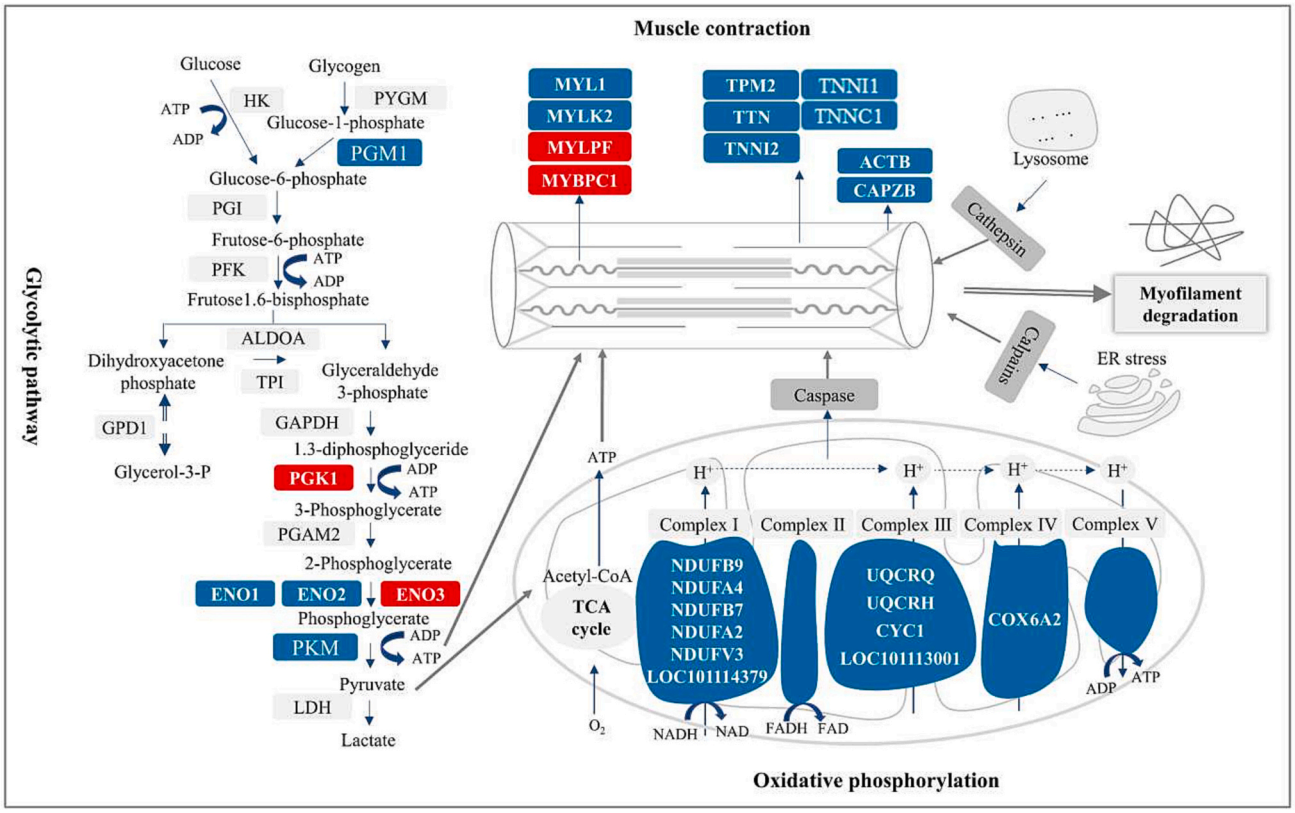

Fig. 5. Summary of the differentially abundant proteins (DAPs) and their biological pathways associated with lamb meat quality in the postmortem. represented the differentially abundant proteins related to meat quality, represented the potential indicators related to raw meat quality.

et al., 2015; Wu, Gao, et al., 2015; Yu et al., 2018). Meanwhile, these reports lacked further validation of the differentially abundant proteins related to meat quality. In the present study, we performed quantitative proteomics analysis for the three DLMQTs groups (with the different tenderness, colour stability and WHC of lamb meat) from 18 LT lamb muscles using TMT proteomics. Subsequently, the differentially abundant proteins were verified by PRM targeted proteomics and western blotting approaches to confirm the potential protein indicators associated with lamb meat quality traits. Three biological pathways were significantly changed in the three DLMQTs groups by proteomics combined with bioinformatic analysis, including glycolysis, oxidative phosphorylation, and muscle contraction. The number of identified dysregulated proteins associated with glycolysis, oxidative phosphorylation and muscle contraction was 11, 20 and 23, respectively. This indicated that the biological pathways of glycolysis, oxidative phosphorylation and muscle contraction can affect the changes in postmortem meat quality.

4.1. Glycolysis

After the bleeding of animals, anaerobic glycolysis continues until glycolytic enzyme inactivation or muscle glycogen depletion. With the progress of glycolysis postmortem, the gradual increase in lactic acid content will lead to a decrease in pH value, ATP synthesis and a series of complex physiological and biochemical changes. In our study, we found 11 dysregulated proteins (HK1, ENO1, ENO2, ENO3, PGM1, PGM2, PGK1, PKM, PGD, PYGL and GFPT1) related to glycolysis among the three DMQTs groups by TMT proteomics. Among them, a total of 8 proteins (ENO1, ENO2, ENO3, PGM1, PGM2, PGK1, PKM, PGD) were downregulated (Fig. 3B). This indicated that glycolysis was inhibited in Group 1 compared to both in Group 2 and Group 3. A previous study also reported that HQ (high-quality) pork meat had lower glycogen content and delayed glycolysis compared to LQ (low-quality) pork (Hou et al., 2020), which is consistent with our results on lamb meat. Moreover, we performed PRM targeted proteomics and western blotting to further verify these dysregulated proteins, and the results showed that the abundance of ENO3, PGK1 and PKM in Group 3 was significantly higher than that in Group 1 and Group 2 ($P < 0.05$, Fig. 4A and C), and PGM1 dramatically decreased protein the levels of in Group 1 compared to Group 3 ($P < 0.05$, Fig. 4A). Enolase (ENO) is one of the key enzymes of glycolysis and can catalyze 2-phosphoglycerate to form phosphoenolpyruvate. In mammals, ENO has three alleles (ENO1, ENO2 and ENO3), and encodes three isozymes (α-enolase, γ-enolase, and β-enolase, respectively) (Kato, Ishiguro, & Ariyoshi, 1983), ENO3 is mainly expressed in muscle tissue. Yu, Wu, Tian, Hou, et al. (2017), Yu, Wu, Tian, Jia, et al. (2017) found that the a^* value of beef was negatively associated with ENO3 abundance during aging, which is consistent with our results. However, Joseph, Suman, Rentfrow, Li, and Beach (2012) reported that ENO3 abundance was positively correlated with the a^* value in *Longissimus lumborum* (LL) of beef compared to *Psoas major* (PM). In addition, the observation showed that compared with the "dark" group (L* value: 43.2 ± 4.6) of pork, the overexpression of ENO3 in the "light" group (L* value: 61.3 ± 2.5) (Sayd et al., 2006). For meat tenderness, previous studies have shown that there was a positive correlation between ENO3 abundance and beef tenderness (Bjarnadóttir et al., 2012; Rosa et al., 2018). Moreover, the study also found that ENO3 decreased the oxidative damage of tender meat compared to that of the tough meat group (Malheiros et al., 2019). Therefore, we inferred that ENO3 is closely related to postmortem meat quality and can be used as a potential marker of meat quality, but it may be affected by species, varieties, oxidative damage, and muscle types. PGK1 is a key metabolic enzyme in the glycolytic pathway that catalyses the conversion of 1,3-diphosphoglyceride to 3-phosphoglycerate and produces the first ATP in glycolysis. The previous study showed that the abundance of PGK1

had a significant impact on drip loss and shear force of pork meat (Kim et al., 2019), which was in agreement with our findings. In addition, the observations found that meat quality is also influenced by the post-translational modification of glycolytic enzymes. For example, Weng et al. (2021) found that the phosphorylated PGK1, PGM1 and PKM proteins were upregulated in the breast muscle of 120-day geese (with the darker and redder meat, chewier and higher WHC) compared to 70–day geese. The dynamic acetylation or deacetylation of glycolytic enzymes, such as ENO3, PGK1, PGM1 and PKM, can regulate the meat quality traits in the conversion of muscle to meat (Jiang, Liu, Shen, Zhou, & Shen, 2019). Moreover, our previous studies also found that protein phosphorylation negatively affects meat quality traits (Li et al., 2021). Therefore, we concluded that glycolysis is one of the key biological pathways during the conversion of muscle to meat, and glycolytic enzymes will regulate the process of glycolysis and then affect postmortem meat quality. In addition, the general linear mixed model analysis showed that the level of PGK1 and ENO3 proteins had a significant impact on shear force, MFI, a^* value, R630/580, cooking loss and drip loss ($P < 0.05$, Table 1). Here, the significantly downregulated glycolytic enzymes (PGK1 and ENO3) may be used as potential indicators for the different lamb meat quality traits. However, the molecular mechanism by which PGK1 and ENO3 proteins regulate meat quality and their relationship with protein posttranslational modification still need to be further investigated.

4.2. Oxidative phosphorylation

The results showed that 20 dysregulated proteins were associated with oxidative phosphorylation and muscle contraction pathways (Fig. 3B). Oxidative phosphorylation is the coupling reaction of ADP and inorganic phosphoric acid to synthesize ATP, and most ATP in organisms comes from oxidative phosphorylation (Nolfi-Donegan, Braganza, & Shiva, 2020). The oxidative phosphorylation system of the mitochondrial inner membrane consists of five enzymes: complex I, complex II, complex III, complex IV and complex V. In the present study, a total of 20 proteins involved in oxidative phosphorylation were identified among three DMQTs groups by TMT proteomics. Among them, 11 proteins, complex I (NDUFB9, NDUFA4, NDUFB7, NDUFA2, NDUFV3, LOC101114379), complex II (UQCRQ, UQCRH, CYC1, LOC101113001) and complex IV (COX6A2), were significantly upregulated in Group 1 compared to Group 2 and Group 3 (Fig. 3B). Yu et al. (2019) reported that oxidative phosphorylation was one of the important biological pathways related to differential beef quality traits of LL and PM muscles using a label-free proteomics strategy, which is consistent with our TMT proteomics findings. We subsequently verified these results by PRM targeted proteomics and western blotting, and the results showed that the abundance of NDUFA2 and NDUFB7 proteins was significantly higher in Group 1 and Group 3 than Group 2 ($P < 0.01$, Fig. 4A and C). It is interesting that NDUFA2 and NDUFB7 proteins only had a significant influence on MFI in model 2 ($P < 0.05$, Table 1). Therefore, whether the differentially abundant proteins of oxidative phosphorylation affect postmortem meat quality, or affect the changes in meat quality through other biological pathways need to be further studied.

4.3. Muscle contraction

In postmortem skeletal muscles, muscle contraction is the sustainable tension development that quickens the interdigitation of sarcomeric thin and thick filaments to an extreme extent, when the exhaustion of ATP and the release of Ca^{2+} from the sarcoplasmic reticulum (Muroya et al., 2007). In our study, we observed that a large number of differentially abundant proteins associated with muscle contraction were upregulated using TMT proteomics. To further verify these results, we performed quantitative analysis of these proteins by western blotting and PRM targeted proteomics, and the results showed that the abundance of seven proteins (MYBPC1, MYPLF, TPM2, TTN, TNNI1, TNNC1 and MYL1) was significantly different among the three DLMQTs groups (Fig. 4A and C). Among them, MYBPC1 and MYPLF showed a significant influence on shear force, MFI, a^* value, R630/580, cooking loss and drip loss by the general linear mixed model ($P < 0.05$, Table 1). Myosin regulatory light chain 2 (MYLPF, skeletal muscle isoform, fast skeletal muscle) encodes fast myosin regulated light chain, which is mainly expressed in fast fibers, and plays an important role in the development of fast and slow skeletal muscle fibers (Schiaffino & Reggiani, 2011). A previous study showed that the anterior region of the porcine *longissimus thoracis et lumborum* muscle had a lower shear force and drip loss and a higher MYLPF abundance (Kim et al., 2019), which is consistent with our results. Gu, Wei, Zhang, and Liu (2020) also reported that MYLPF was positively correlated with a^* value of lamb meat. Hence, MYLPF may be used as a potential indicator for meat quality, we inferred that this may be related to MYLPF being involved in cytoskeleton composition and influencing the type composition of muscle fibers, affecting meat quality. However, whether MYLPF can really be used as an indicator to characterize meat quality and its characterization mechanism need to be further investigated. MYBPC1 (myosin-binding protein C, slow-type) is a major myosin-binding protein isoform in vertebrate striated skeletal muscle that plays an important role in effective energy metabolism, muscle contraction and relaxation (Chen et al., 2011). The previous study found that MYBPC1 is positively related to marbling of intramuscular fat of Japanese Black beef cattle (Tong et al., 2014). Moreover, the findings also showed that myosin light chains can affect the glycolytic rate postmortem (Choi, Ryu, & Kim, 2007).

5. Conclusion

Proteomics analysis is a valuable and powerful tool that provides a comprehensive understanding of the difference in lamb meat quality traits postmortem. In this study, we quantified 2176 proteins in three different lamb meat quality groups by TMT proteomics. Among them, 4 dysregulated proteins (ENO3, PGK1, MYBPC1 and MYLPF) were verified to be associated with meat quality by PRM targeted proteomics and western blotting approaches, which may be used as potential indicators to assess and characterize the postmortem lamb meat quality. The molecular biological pathways suggested that glycolysis, oxidative phosphorylation and muscle contraction remarkably changed in different meat quality groups, and were the key pathways influencing postmortem meat quality. Therefore, this study will provide an important molecular basis for understanding the mechanism of postmortem meat quality, and offer a reference for developing regulation technology and detection technology to improve lamb meat quality in the future.

CRediT authorship contribution statement

Caiyan Huang: Conceptualization, Methodology, Software, Writing – original draft, Writing – review & editing. **Christophe Blecker:** Supervision. **Li Chen:** Investigation. **Can Xiang:** Methodology, Formal analysis. **Xiaochun Zheng:** Data curation, Resources. **Zhenyu Wang:** Investigation, Validation, Supervision. **Dequan Zhang:** Investigation, Validation, Supervision.

Declaration of Competing Interest

The authors declare that they have no known competing financial interests or personal relationships that could have appeared to influence the work reported in this paper.

Data availability

The authors do not have permission to share data.

Acknowledgements

This study was funded by the Key R&D projects of the Ningxia Hui Autonomous Region, China (NO 2021BBF02037), and Agricultural Science and Technology Innovation Program, Institute of Food Science and Technology, Chinese Academy of Agricultural Sciences (CAAS-ASTIP-2022-IFST). We thank Mr. Chongxing Mo for his support of ASReml-R data analysis.

Appendix A. Supplementary data

Supplementary data to this article can be found online at https://doi.org/10.1016/j.meatsci.2023.109126.

References

Beldarrain, L. R., Aldai, N., Picard, B., Sentandreu, E., Navarro, J. L., & Sentandreu, M. A. (2018). Use of liquid isoelectric focusing (OFFGEL) on the discovery of meat tenderness biomarkers. *Journal of Proteomics, 183*, 25–33. https://doi.org/10.1016/j.jprot.2018.05.005

Bjarnadóttir, S. G., Hollung, K., Høy, M., Bendixen, E., Codrea, M. C., & Veiseth-Kent, E. (2012). Changes in protein abundance between tender and tough meat from bovine longissimus thoracis muscle assessed by isobaric tag for relative and absolute quantitation (iTRAQ) and 2-dimensional gel electrophoresis analysis. *Journal of Animal Science, 90*(6), 2035–2043. https://doi.org/10.2527/jas.2011-4721

Boudon, S., Ounaissi, D., Viala, D., Monteils, V., Picard, B., & Cassar-Malek, I. (2020). Label free shotgun proteomics for the identification of protein biomarkers for beef tenderness in muscle and plasma of heifers. *Journal of Proteomics, 217*, Article 103685. https://doi.org/10.1016/j.jprot.2020.103685

Butler, D. (2009). *Asreml: Asreml fits the linear mixed model. R Package Version. 3*.

Chauhan, S. S., & England, E. M. (2018). Postmortem glycolysis and glycogenolysis: Insights from species comparisons. *Meat Science, 144*, 118–126. https://doi.org/10.1016/j.meatsci.2018.06.021

Chen, Z., Zhao, T.-J., Li, J., Gao, Y.-S., Meng, F.-G., Yan, Y.-B., & Zhou, H.-M. (2011). Slow skeletal muscle myosin-binding protein-C (MyBPC1) mediates recruitment of muscle-type creatine kinase (CK) to myosin. *Biochemical Journal, 436*(2), 437–445. https://doi.org/10.1042/bj20102007

Choi, Y. M., Ryu, Y. C., & Kim, B. C. (2007). Influence of myosin heavy- and light chain isoforms on early postmortem glycolytic rate and pork quality. *Meat Science, 76*(2), 281–288. https://doi.org/10.1016/j.meatsci.2006.11.009

Fuente-Garcia, C., Aldai, N., Sentandreu, E., Oliván, M., García-Torres, S., Franco, D., … Sentandreu, M. A. (2019). Search for proteomic biomarkers related to bovine pre-slaughter stress using liquid isoelectric focusing (OFFGEL) and mass spectrometry. *Journal of Proteomics, 198*, 59–65. https://doi.org/10.1016/j.jprot.2018.10.013

Gu, M., Wei, Y., Zhang, D., & Liu, Y. (2020). iTRAQ based proteomic profile analysis for goat longissimus thoracis under repeated freeze-thaw treatments. *LWT, 134*, Article 109934. https://doi.org/10.1016/j.lwt.2020.109934

Hopkins, D. L., Toohey, E. S., Warner, R. D., Kerr, M. J., & van de Ven, R. (2010). Measuring the shear force of lamb meat cooked from frozen samples: Comparison of two laboratories. *Animal Production Science, 50*(6), 382–385. https://doi.org/10.1071/AN09162

Hou, X., Liu, Q., Meng, Q., Wang, L., Yan, H., Zhang, L., & Wang, L. (2020). TMT-based quantitative proteomic analysis of porcine muscle associated with postmortem meat quality. *Food Chemistry, 328*, Article 127133. https://doi.org/10.1016/j.foodchem.2020.127133

Huang, C., Hou, C., Ijaz, M., Yan, T., Li, X., Li, Y., & Zhang, D. (2020). Proteomics discovery of protein biomarkers linked to meat quality traits in post-mortem muscles: Current trends and future prospects: A review. *Trends in Food Science & Technology, 105*, 416–432. https://doi.org/10.1016/j.tifs.2020.09.030

Jiang, S., Liu, Y., Shen, Z., Zhou, B., & Shen, Q. W. (2019). Acetylome profiling reveals extensive involvement of lysine acetylation in the conversion of muscle to meat. *Journal of Proteomics, 205*, Article 103412. https://doi.org/10.1016/j.jprot.2019.103412

Jin, S., Pang, Q., Yang, H., Diao, X., Shan, A., & Feng, X. (2021). Effects of dietary resveratrol supplementation on the chemical composition, oxidative stability and meat quality of ducks (Anas platyrhynchos). *Food Chemistry, 363*, Article 130263. https://doi.org/10.1016/j.foodchem.2021.130263

Joseph, P., Suman, S. P., Rentfrow, G., Li, S., & Beach, C. M. (2012). Proteomics of muscle-specific beef color stability. *Journal of Agricultural and Food Chemistry, 60*(12), 3196–3203. https://doi.org/10.1021/jf204188v

Kato, K., Ishiguro, Y., & Ariyoshi, Y. (1983). Enolase isozymes as disease markers: Distribution of three enolase subunits (α, β, and γ) in various human tissues. [article]. *Disease Markers, 1*(3), 213–220.

Kenward, M. G., & Roger, J. H. (1997). Small sample inference for fixed effects from restricted maximum likelihood. *Biometrics, 53*(3), 983–997.

Kim, G.-D., Jeong, J.-Y., Yang, H.-S., & Hur, S. J. (2019). Differential abundance of proteome associated with intramuscular variation of meat quality in porcine longissimus thoracis et lumborum muscle. *Meat Science, 149*, 85–95. https://doi.org/10.1016/j.meatsci.2018.11.012

Koohmaraie, M., & Geesink, G. H. (2006). Contribution of postmortem muscle biochemistry to the delivery of consistent meat quality with particular focus on the calpain system. *Meat Science, 74*(1), 34–43. https://doi.org/10.1016/j.meatsci.2006.04.025

Li, X., Zhang, D., Ren, C., Bai, Y., Ijaz, M., Hou, C., & Chen, L. (2021). Effects of protein posttranslational modifications on meat quality: A review. *Comprehensive Reviews in Food Science and Food Safety, 20*(1), 289–331. https://doi.org/10.1111/1541-4337.12668

Ma, D., & Kim, Y. H. B. (2020). Proteolytic changes of myofibrillar and small heat shock proteins in different bovine muscles during aging: Their relevance to tenderness and water-holding capacity. *Meat Science, 163*. https://doi.org/10.1016/j.meatsci.2020.108090

Malheiros, J. M., Braga, C. P., Grove, R. A., Ribeiro, F. A., Calkins, C. R., Adamec, J., & Chardulo, L. A. L. (2019). Influence of oxidative damage to proteins on meat tenderness using a proteomics approach. *Meat Science, 148*, 64–71. https://doi.org/10.1016/j.meatsci.2018.08.016

Muroya, S., Ohnishi-Kameyama, M., Oe, M., Nakajima, I., Shibata, M., & Chikuni, K. (2007). Double phosphorylation of the myosin regulatory light chain during rigor mortis of bovine longissimus muscle. *Journal of Agricultural and Food Chemistry, 55*(10), 3998–4004.

Nakagawa, S., & Schielzeth, H. (2013). A general and simple method for obtaining R2 from generalized linear mixed-effects models. *Methods in Ecology and Evolution, 4*(2), 133–142. https://doi.org/10.1111/j.2041-210x.2012.00261.x

Nolfi-Donegan, D., Braganza, A., & Shiva, S. (2020). Mitochondrial electron transport chain: Oxidative phosphorylation, oxidant production, and methods of measurement. *Redox Biology, 37*, Article 101674. https://doi.org/10.1016/j.redox.2020.101674

R Core Team. (2014). *R: A language and environment for statistical computing*. Vienna, Austria: R Foundation for Statistical Computing. http://www.R-project.org/.

Rajagopal, K., & Oommen, G. T. (2015). Myofibril fragmentation index as an immediate postmortem predictor of Buffalo meat tenderness. *Journal of Food Processing and Preservation, 39*(6), 1166–1171. https://doi.org/10.1111/jfpp.12331

Rosa, A. F., Moncau, C. T., Poleti, M. D., Fonseca, L. D., Balieiro, J. C. C., Silva, S. L. E., & Eler, J. P. (2018). Proteome changes of beef in Nellore cattle with different genotypes for tenderness. *Meat Science, 138*, 1–9. https://doi.org/10.1016/j.meatsci.2017.12.006

Sayd, T., Morzel, M., Chambon, C., Franck, M., Figwer, P., Larzul, C., … Laville, E. (2006). Proteome analysis of the sarcoplasmic fraction of pig semimembranosus muscle: Implications on meat color development. *Journal of Agricultural and Food Chemistry, 54*(7), 2732–2737. https://doi.org/10.1021/jf052569v

Schiaffino, S., & Reggiani, C. (2011). Fiber types in mammalian skeletal muscles. *Physiological Reviews, 91*(4), 1447–1531. https://doi.org/10.1152/physrev.00031.2010

Silva, L. H. P., Rodrigues, R. T. S., Assis, D. E. F., Benedeti, P. D. B., Duarte, M. S., & Chizzotti, M. L. (2019). Explaining meat quality of bulls and steers by differential proteome and phosphoproteome analysis of skeletal muscle. *Journal of Proteomics, 199*, 51–66. https://doi.org/10.1016/j.jprot.2019.03.004

Starkey, C. P., Geesink, G. H., Collins, D., Hutton Oddy, V., & Hopkins, D. L. (2016). Do sarcomere length, collagen content, pH, intramuscular fat and desmin degradation explain variation in the tenderness of three ovine muscles? *Meat Science, 113*, 51–58. https://doi.org/10.1016/j.meatsci.2015.11.013

Starkey, C. P., Geesink, G. H., van de Ven, R., & Hopkins, D. L. (2017). The relationship between shear force, compression, collagen characteristics, desmin degradation and sarcomere length in lamb biceps femoris. *Meat Science, 126*, 18–21. https://doi.org/10.1016/j.meatsci.2016.12.006

Tong, B., Sasaki, S., Muramatsu, Y., Ohta, T., Kose, H., Yamashiro, H., … Yamada, T. (2014). Association of a single-nucleotide polymorphism in myosin-binding protein C, slow-type (MYBPC1) gene with marbling in Japanese black beef cattle. *Animal Genetics, 45*(4), 611–612. https://doi.org/10.1111/age.12172

Weng, K., Huo, W., Gu, T., Bao, Q., Cao, Z., Zhang, Y., … Chen, G. (2021). Quantitative phosphoproteomic analysis unveil the effect of marketable ages on meat quality in geese. *Food Chemistry, 361*, Article 130093. https://doi.org/10.1016/j.foodchem.2021.130093

Willimas, P. (2007). Nutritional composition of red meat. *Nutrition & Dietetics, 64*(s4), S113–S119. https://doi.org/10.1111/j.1747-0080.2007.00197.x

Wu, W., Fu, Y., Therkildsen, M., Li, X.-M., & Dai, R.-T. (2015). Molecular understanding of meat quality through application of proteomics. *Food Reviews International, 31*(1), 13–28. https://doi.org/10.1080/87559129.2014.961073

Wu, W., Gao, X.-G., Dai, Y., Fu, Y., Li, X.-M., & Dai, R.-T. (2015). Post-mortem changes in sarcoplasmic proteome and its relationship to meat color traits in M. semitendinosus of Chinese Luxi yellow cattle. *Food Research International, 72*, 98–105. https://doi.org/10.1016/j.foodres.2015.03.030

Yu, Q., Tian, X., Shao, L., Xu, L., Dai, R., & Li, X. (2018). Label-free proteomic strategy to compare the proteome differences between longissimus lumborum and psoas major muscles during early postmortem periods. *Food Chemistry, 269*, 427–435. https://doi.org/10.1016/j.foodchem.2018.07.040

Yu, Q., Tian, X., Sun, C., Shao, L., Li, X., & Dai, R. (2019). Comparative transcriptomics to reveal muscle-specific molecular differences in the early postmortem of Chinese Jinjiang yellow cattle. *Food Chemistry, 301*, Article 125262. https://doi.org/10.1016/j.foodchem.2019.125262

Yu, Q., Wu, W., Tian, X., Hou, M., Dai, R., & Li, X. (2017). Unraveling proteome changes of Holstein beef M. semitendinosus and its relationship to meat discoloration during post-mortem storage analyzed by label-free mass spectrometry. *Journal of Proteomics, 154*, 85–93. https://doi.org/10.1016/j.jprot.2016.12.012

Yu, Q., Wu, W., Tian, X., Jia, F., Xu, L., Dai, R., & Li, X. (2017). Comparative proteomics to reveal muscle-specific beef color stability of Holstein cattle during post-mortem

storage. *Food Chemistry, 229*, 769–778. https://doi.org/10.1016/j.foodchem.2017.03.004

Zhang, M., Wang, D., Huang, W., Liu, F., Zhu, Y., Xu, W., & Cao, J. (2013). Apoptosis during postmortem conditioning and its relationship to duck meat quality. *Food Chemistry, 138*(1), 96–100. https://doi.org/10.1016/j.foodchem.2012.10.142

Zhang, M., Wang, D., Xu, X., & Xu, W. (2019). Comparative proteomic analysis of proteins associated with water holding capacity in goose muscles. *Food research international (Ottawa, Ont.), 116*, 354–361. https://doi.org/10.1016/j.foodres.2018.08.048